

Finite Element Modeling of Human Femur Diaphysis

George E. Henderson, Emma H. Conard and Joseph L. Palladino
Department of Engineering, Trinity College, Hartford, CT 06106, USA

Abstract—Modeling biological structures is challenging due to their often complex anatomical geometries and material properties. Finite element studies of the femur, the largest and strongest bone in the human body, have focused on the femoral neck, since this is where fractures often occur. This study developed COMSOL finite element models of the human femur diaphysis (shaft), subjected to anatomical loading. Models were developed from a simple, hollow cylinder; to an anatomical, but uniform, cross section; to an anatomically correct model with eleven cross sections. Models were subjected to physiologically relevant axial, torsional, and bending loads. The calculated stresses and deformations were used to quantitatively compare the models. Results show the importance of anatomical geometry in biomechanical models.

Keywords: Femur diaphysis, anatomical cross sections, COMSOL Multiphysics, 3D lofting of profiles, solid mechanics, axial compression, torsion, bending, von Mises stresses, deflections.

I. METHODS

1) *Equations:* Solid modeling requires three equations: an equilibrium balance, a constitutive relation relating stress and strain, and a kinematic relation relating displacement to strain. Newton's second law serves as the equilibrium equation, which in tensor form is

$$\nabla \cdot \boldsymbol{\sigma} + \mathbf{F}_v = \rho \ddot{\mathbf{u}} \quad (1)$$

where $\boldsymbol{\sigma}$ is stress, \mathbf{F}_v is body force per volume, ρ is density, and $\ddot{\mathbf{u}}$ is acceleration. For static analysis, the right-hand side of this equation goes to zero.

The constitutive equation relating the stress tensor $\boldsymbol{\sigma}$ to strain $\boldsymbol{\epsilon}$ is the generalized Hooke's law

$$\boldsymbol{\sigma} = \mathbf{C} : \boldsymbol{\epsilon} \quad (2)$$

where \mathbf{C} is the fourth-order elasticity tensor. In COMSOL, this relation is expanded to

$$\boldsymbol{\sigma} - \boldsymbol{\sigma}_0 = \mathbf{C} : (\boldsymbol{\epsilon} - \boldsymbol{\epsilon}_0 - \boldsymbol{\epsilon}_{inel}) \quad (3)$$

For this application, initial stress $\boldsymbol{\sigma}_0$, initial strain $\boldsymbol{\epsilon}_0$, and inelastic strain $\boldsymbol{\epsilon}_{inel}$ are all zero. For isotropic

material, the elasticity tensor reduces to the 6×6 elasticity matrix

$$\begin{bmatrix} 2\mu + \lambda & \lambda & \lambda & 0 & 0 & 0 \\ \lambda & 2\mu + \lambda & \lambda & 0 & 0 & 0 \\ \lambda & \lambda & 2\mu + \lambda & 0 & 0 & 0 \\ 0 & 0 & 0 & \mu & 0 & 0 \\ 0 & 0 & 0 & 0 & \mu & 0 \\ 0 & 0 & 0 & 0 & 0 & \mu \end{bmatrix} \quad (4)$$

where λ and μ are the Lamé constants. Material properties for cortical bone are listed in Table I.

The final required equation is the kinematic relation between displacements \mathbf{u} and strains $\boldsymbol{\epsilon}$. In tensor form

$$\boldsymbol{\epsilon} = \frac{1}{2} [\nabla \mathbf{u} + (\nabla \mathbf{u})^T] \quad (5)$$

For rectangular Cartesian coordinates, the strain tensor may be written in indicial notation [1]

$$\epsilon_{ij} = \frac{1}{2} \left[\frac{\partial u_j}{\partial x_i} + \frac{\partial u_i}{\partial x_j} + \frac{\partial u_\alpha}{\partial x_i} \frac{\partial u_\alpha}{\partial x_j} \right] \quad (6)$$

where $\alpha = 1, 2, 3, \dots$. For small deformations the higher order terms are negligible and ϵ_{ij} reduces to Cauchy's infinitesimal strain tensor

$$\epsilon_{ij} = \frac{1}{2} \left[\frac{\partial u_j}{\partial x_i} + \frac{\partial u_i}{\partial x_j} \right] \quad (7)$$

TABLE I
MATERIAL PROPERTIES FOR CORTICAL BONE [2].

Parameter	Symbol	Value
Elastic Modulus	E	17.9 GPa
Poisson's Ratio	ν	0.39
Density	ρ	1908 kg/m ³

2) *COMSOL Multiphysics Model*: Anatomical femur cross sections were built using medical CT scan data from the literature [3]. Data points defining the outer perimeter (periosteum) and inner perimeter (endosteum) were digitized from these scans. The first anatomical model in the present study used the cross section at 50% of femur length, extruded, giving a prismatic anatomical model. Subsequently, work planes were defined for the outer perimeter, and the inner perimeter, for each of the 11 femur cross sections, for a total of 22 work planes. The 11 outer perimeter profiles were contoured by vertex projection and then lofted into a 3D solid. Similarly for the 11 inner perimeter profiles. Vertices were projected to prevent twisting along the femur long axis. The interior lofted solid was then subtracted from the exterior lofted solid, giving the final geometry.

The models were constrained at one end and loaded at the other for the three cases of axial compression, torsion, and bending. A combined bending load using a normal caput-collum-diaphyseal (CCD) angle of 130° and one half of a 70 kg body mass was also applied. A very fine or extremely fine ($3.8E6$ degrees of freedom) physics-controlled mesh was generated and a stationary analysis was performed, using default solver settings. The model used isotropic material properties of cortical bone with elastic modulus of 17.4 GPa, Poisson's ratio of 0.39, and density of 1908 kg/m³.

II. RESULTS

Figures 1 to 3 are diaphysis cross sections at 1%, 50%, and 100%, respectively, showing the high degree of anatomical variation at different locations. For each cross section, orientation is anterior/posterior (top/bottom) and medial/lateral (left/right). The area bounded by the red interpolation curve is total area TotA. The area bounded by the green interpolation curve is medullary area, MedA, and the difference is cortical area, CA. Table II shows for each section, taken as a percentage of femur length L, total area TotA, medullary area MedA, and cortical area CA, as well as mean values for each.

A. Axial Compression

Femur models were fixed at the distal end and loaded with a physiologically realistic axial compressive load

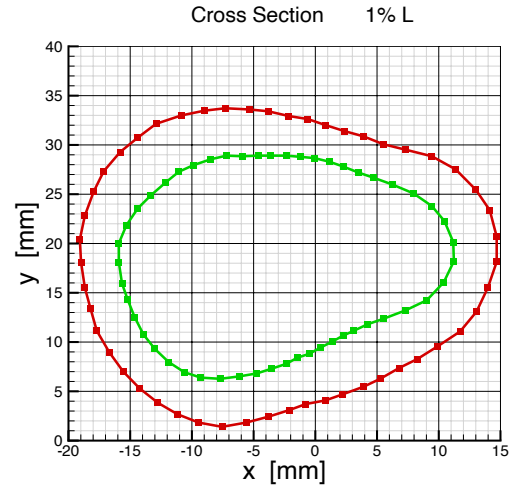


Fig. 1. Cross section at 1% of femur length.

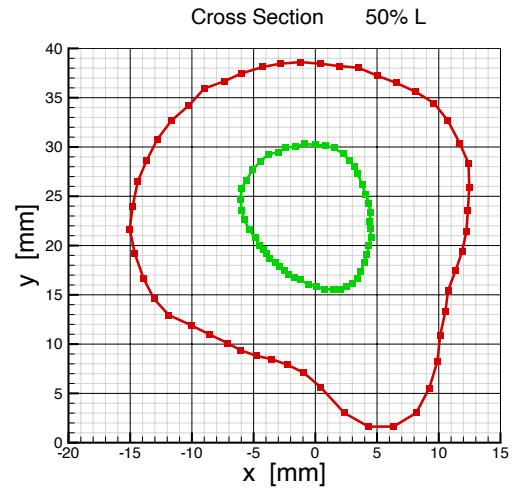


Fig. 2. Cross section at 50% of femur length.

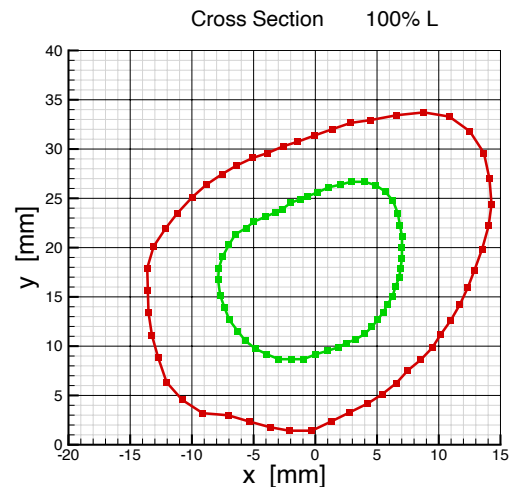


Fig. 3. Cross section at 100% of femur length.

TABLE II

FEMUR DIAPHYSIS CROSS SECTIONAL AREAS. PERCENTAGE FEMUR LENGTH %L, TOTAL AREA TOTA, MEDULLARY AREA MEDA, AND CORTICAL AREA CA.

%L	TotA	MedA	CA
1	823	454	369
10	797	372	425
20	770	273	497
30	688	174	514
40	664	138	526
50	738	118	620
60	718	93	625
70	751	90	661
80	783	120	663
90	692	140	552
100	665	201	464
mean	735	198	537

of 70 kg/2 at the proximal end. Maximum von Mises stress for the solid and hollow cylinder models agree with hand calculations (not shown). Maximum von Mises stress for the one-section anatomical model were also as expected (load/cross section). Figure 4 shows the full femur model subjected to axial compressive loading. Note that there are three high stress areas that arise due to the non prismatic nature of this model. Table III summarizes maximum von Mises stress and maximum displacement for each of the four models. For all, maximum stress is below the ultimate compressive, longitudinal stress for cortical bone, 195 MPa, and displacement is negligible.

TABLE III

MAXIMUM VON MISES STRESS AND MAXIMUM DISPLACEMENT FOR EACH OF THE FOUR FEMUR MODELS WITH AXIAL COMPRESSION LOADING.

Model	max σ_{vm} [MPa]	max displacement [mm]
solid	0.467	0.0102
hollow	0.639	0.0139
1 section	0.554	0.0121
full 11 section	≈ 2	0.1346

B. Torsion

The four femur models were loaded with a 200 Nm load at the distal end. This load does not correspond to normal physiological conditions, but might arise,

for example, by a torque produced at the end of a ski. Again, results for the solid and hollow cylinder models agree with hand calculations and are not shown. As expected, von Mises stresses for these two models is uniform for a given radius. Table IV summarizes maximum von Mises stress and maximum displacement for each of the four models.

Figure 5 shows von Mises stresses for the one section model. The longitudinal red strip shows a high stress region arising from the asymmetric anatomical cross section. Stress in this region is 127 MPa, which exceeds the ultimate shear stress for cortical bone, 69 MPa. Maximum displacement for this model is 3.52 mm.

Figure 6 shows von Mises stresses for the full 11 section femur model. High stress regions arise from the anatomical structure, with peak of 148 MPa, far exceeding the ultimate shear stress for cortical bone of 69 MPa. Maximum displacement for this model is 3.53 mm, virtually the same as for the one section model.

TABLE IV

MAXIMUM VON MISES STRESS AND MAXIMUM DISPLACEMENT FOR EACH OF THE FOUR FEMUR MODELS WITH 200 NM TORSIONAL LOADING. THE ANATOMICAL MODELS BOTH SHOW VON MISES STRESSES THAT EXCEED 69 MPa, THE ULTIMATE SHEAR STRESS FOR CORTICAL BONE.

Model	max σ_{vm} [MPa]	max displacement [mm]
solid	61.7	2.16
hollow	66.4	2.33
1 section	127	3.52
full 11 section	148	3.53

C. Bending

The four femur models were loaded with a 200 N transverse load at the distal end. This load does not correspond to normal physiological conditions, but might arise, for example, by the lower leg being fixed by terrain and the upper body continuing to move forward in three-point bending, as in a so-called “boot top” fracture. Once again, results for the solid and hollow cylinder models agree with hand calculations and are not shown. Table V summarizes maximum von Mises stress and maximum displacement for each of the four models. For all four models, maximum von

Volume: von Mises stress (N/m²)

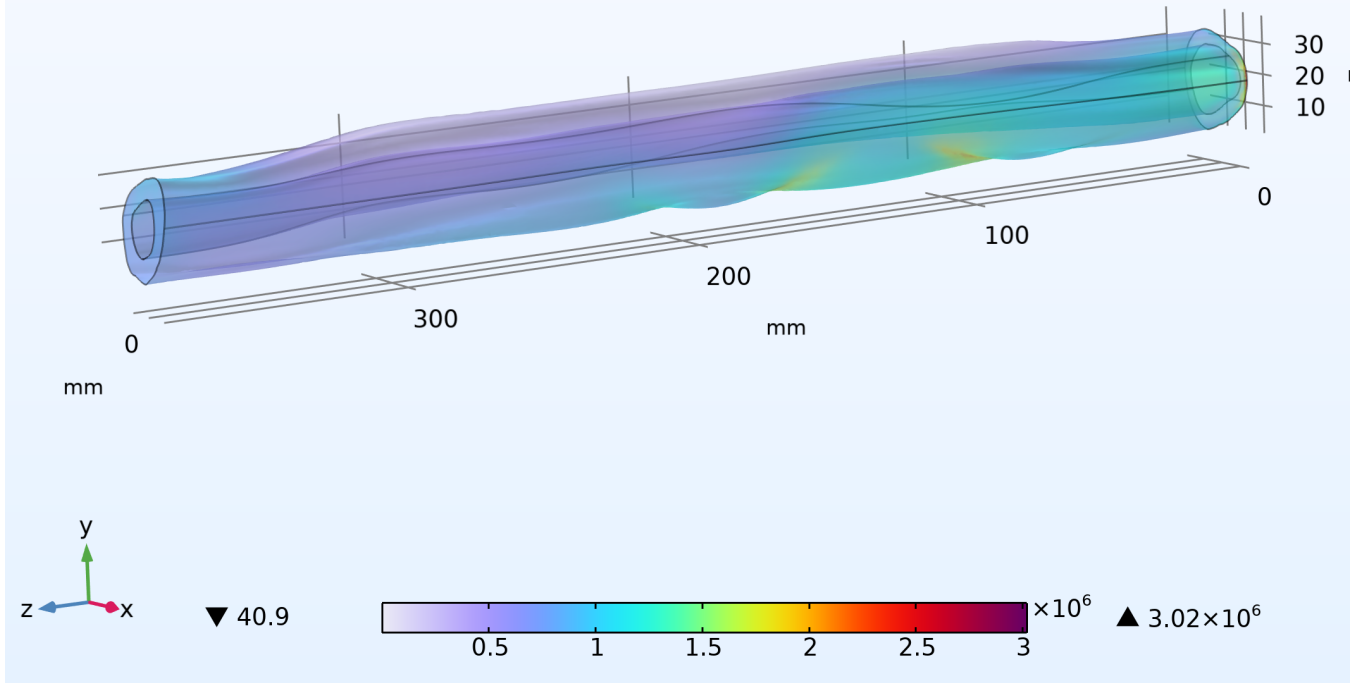


Fig. 4. Von Mises stress calculated for a compressive axial load of one half 70 kg body mass applied to the full, 11 section anatomical femur model.

Mises stress was below the ultimate bending normal stress for cortical bone, 209 MPa.

Figure 7 shows von Mises stresses for the one section model subjected to a bending load. The asymmetric cross section leads this model to be more resistant to bending in the anterior/posterior direction than the medial/lateral direction. Maximum displacement for this model is 3.89 mm for the former and 6.20 mm for the latter.

Figure 8 shows von Mises stresses for the full 11 section femur model subjected to bending. The asymmetric cross section leads this model to be more resistant to bending in the anterior/posterior direction than the medial/lateral direction. Maximum displacement for this model is 4.60 mm for the former and 10.9 mm for the latter. Loading in the medial/lateral direction (not shown) produces maximum von Mises stress of 153 MPa, which starts to approach the ultimate bending

normal stress of 209 MPa for cortical bone.

TABLE V
MAXIMUM VON MISES STRESS AND MAXIMUM DISPLACEMENT FOR EACH OF THE FOUR FEMUR MODELS FOR A BENDING LOAD OF 200 N APPLIED TO THE DISTAL END.

Model	max σ_{vm} [MPa]	max displacement [mm]
solid	36.7	4.87
hollow	40.8	5.28
1 section	61.4	3.89
full 11 section	75.5	4.60

Volume: von Mises stress (N/m²)

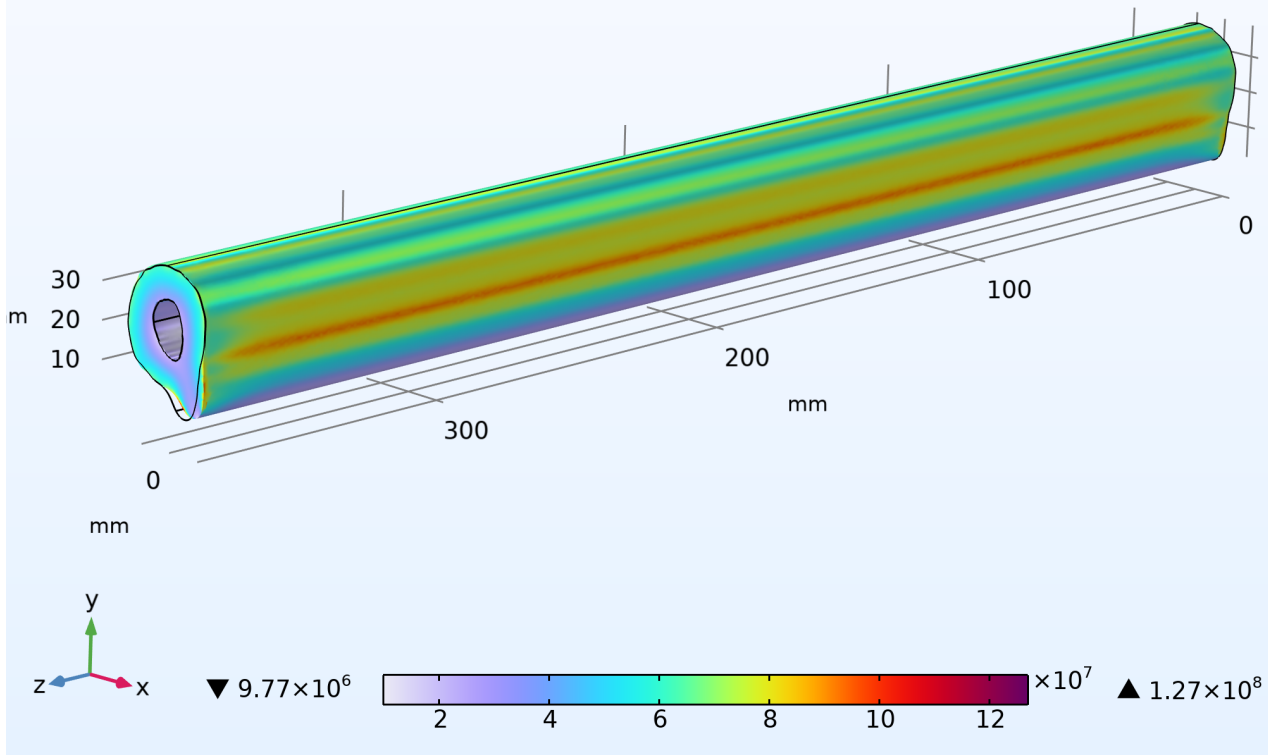


Fig. 5. Von Mises stress calculated for a 200 Nm torsion load applied to the one section anatomical femur model.

III. DISCUSSION AND CONCLUSIONS

Modeling biological structures is challenging due to their complicated geometries. This study modeled the human femur diaphysis with increasingly complex geometric models, starting with a solid cylinder and a hollow cylinder. The mid-length cross section from a femur CT scan was then used to extrude a femur shaft with a uniform anatomical cross section. Finally, 11 femur cross section CT scans were used to define 22 work planes with interpolation functions describing the outer (periosteum) and inner (endosteum) cross section perimeters, resulting in a nonuniform anatomical model.

Results show that taking into account anatomical geometry significantly affects FEA analysis of the femur shaft. Even for axial compression, unexpected high stress regions arise from the non-prismatic nature of the anatomical model. For torsion and bending loads,

differences between the simple and anatomical models was even more significant.

Future work should consider bone's anisotropic properties. In addition to having different elastic moduli in the transverse and longitudinal directions, bone is much stronger in compression than in tension.

Volume: von Mises stress (N/m²) Mesh

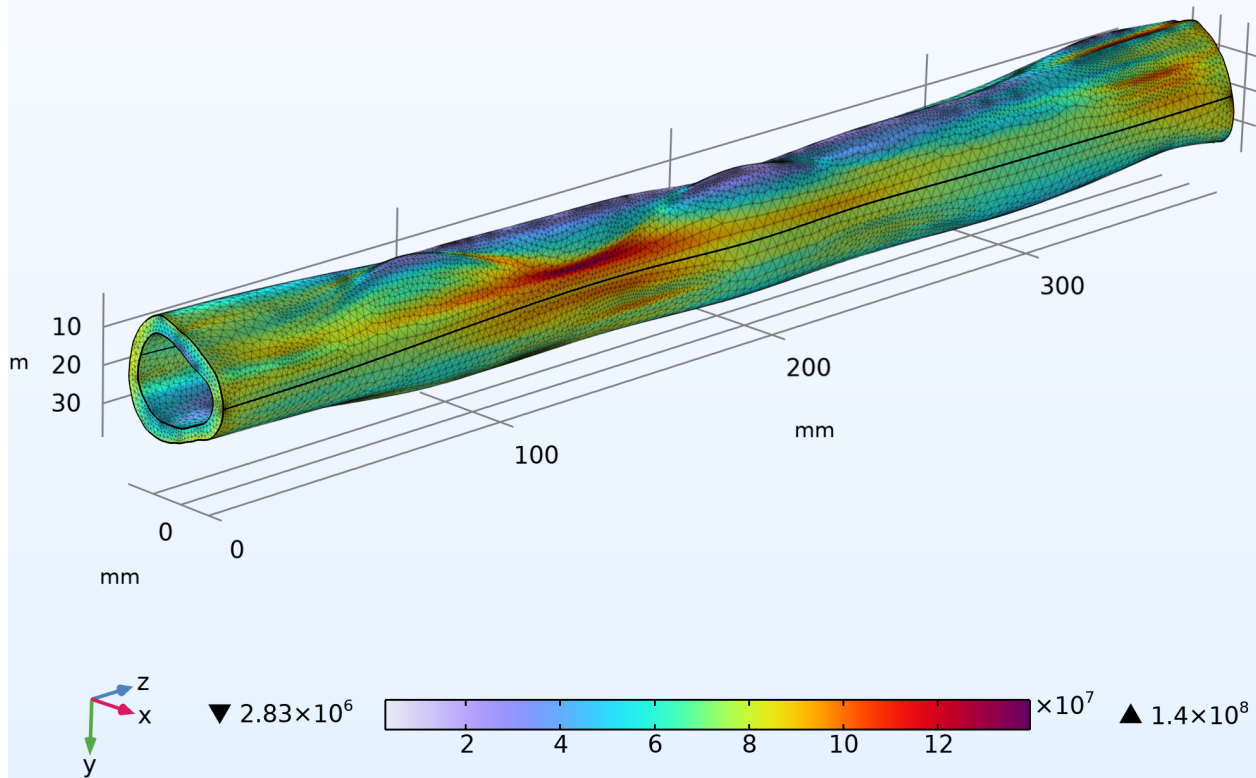


Fig. 6. Von Mises stress calculated for a 200 Nm torsion load applied to the full 11 section anatomical femur model. The high stress regions exceed the ultimate shear stress of 69 MPa for cortical bone.

REFERENCES

- [1] Fung, Y.C., *A First Course in Continuum Mechanics (2ed)*, Prentice-Hall, Englewood Cliffs, NJ, 1977.
- [2] R. B. Martin, et al., *Mechanical Properties of Bone*, chapter. 7 in: *Skeletal Tissue Mechanics (2ed)*, Springer, NY, 2015.
- [3] A. Proficio, et al., morphomap: An R package for long bone landmarking, cortical thickness, and cross-sectional geometry mapping, *Am. J. Phys. Anthro.* 174(1):129—139, 2021.
- [4] Z. Yang, *Finite Element Analysis for Biomedical Engineering Applications*, CRC Press, FL, 2019.

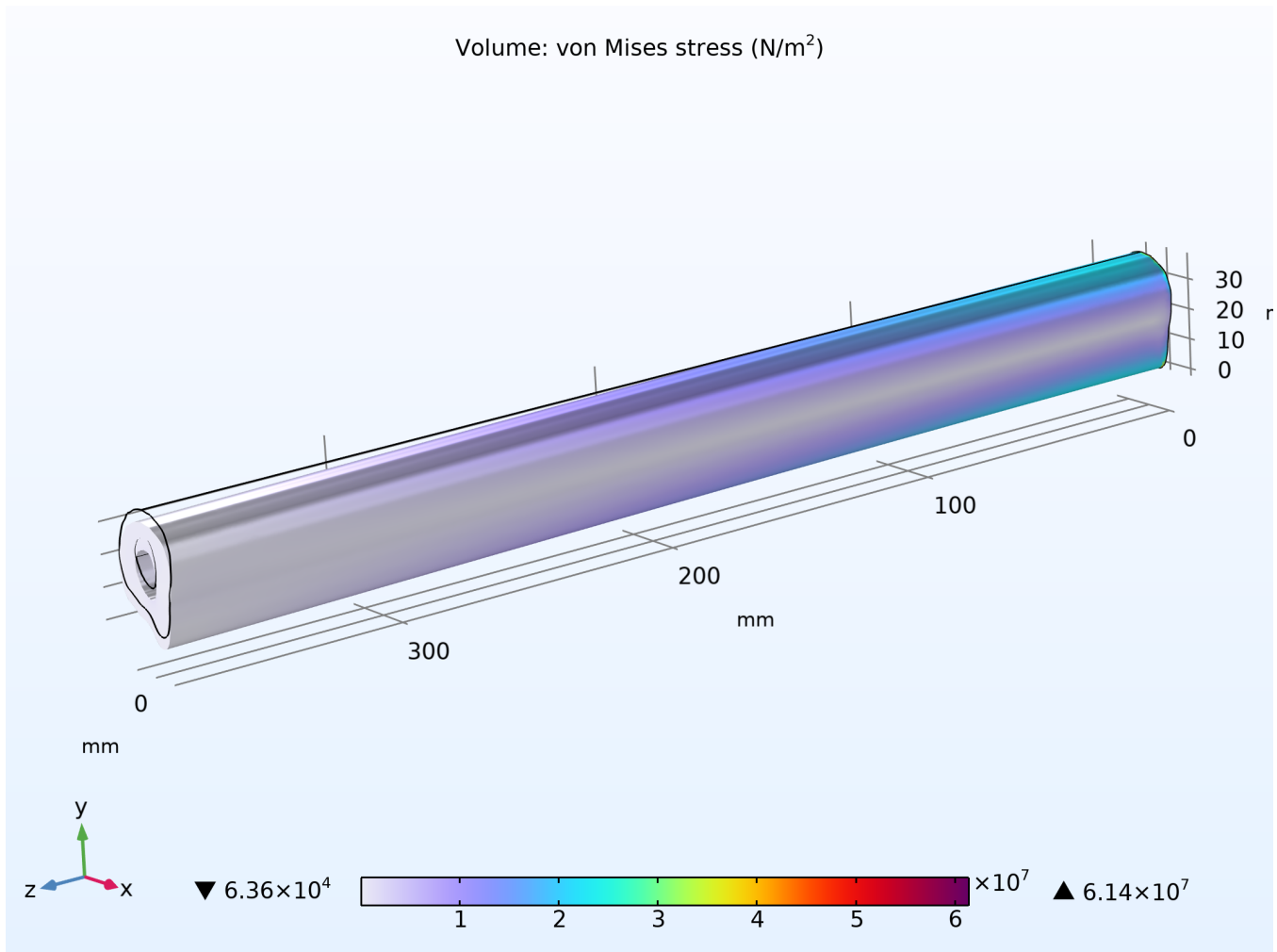


Fig. 7. Maximum von Mises stresses for the one section femur model subjected to a bending load. The asymmetric cross section leads this model to be more resistant to bending in the anterior/posterior direction than the medial/lateral direction.

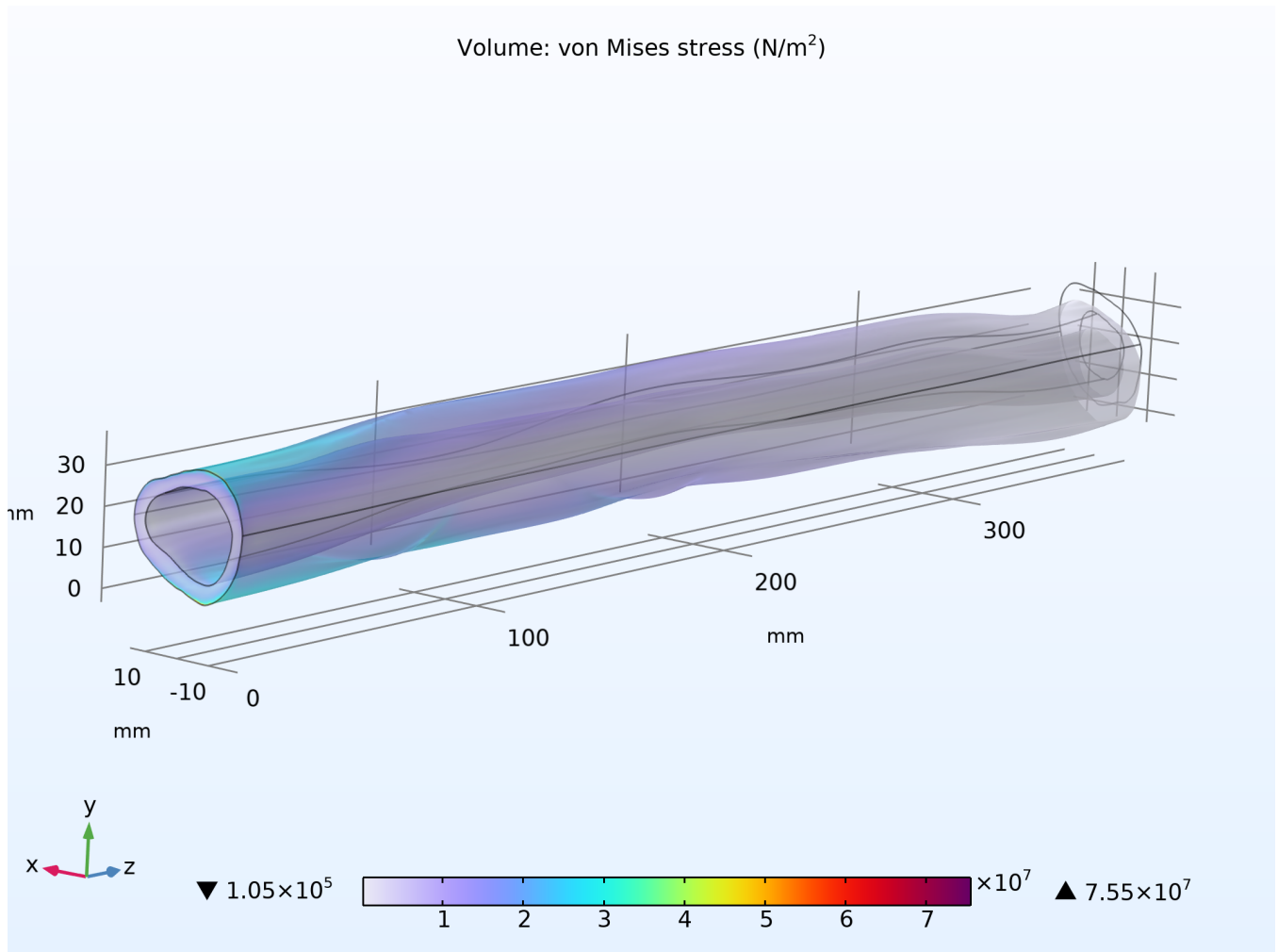


Fig. 8. Maximum von Mises stresses for the full 11 section femur model subjected to a bending load. The asymmetric cross section leads this model to be more resistant to bending in the anterior/posterior direction than the medial/lateral direction.